

Hydrogen plasma enhanced crystallization of hydrogenated amorphous silicon films

K. Pangal,^{a)} J. C. Sturm,^{b)} and S. Wagner

Department of Electrical Engineering, Princeton University, Princeton, New Jersey 08544

T. H. Büyüklihanli

Evan East, 666 Plainsboro Road, Plainsboro, New Jersey 08536

(Received 25 August 1998; accepted for publication 21 October 1998)

We report that a room temperature hydrogen plasma exposure in a parallel plate diode type reactive ion etcher can reduce the time required for the subsequent thermal crystallization of amorphous silicon time by a factor of five. Exposure to hydrogen plasma reduces the incubation time, while the rate of crystallization itself is not greatly affected. This plasma enhanced crystallization can be spatially controlled by masking with patterned oxide, so that both amorphous and polycrystalline areas can be realized simultaneously at desired locations on a single substrate. The enhancement of crystallization rate is probably due to the creation of seed nuclei at the surface. The films have been characterized by UV reflectance, x-ray diffraction, plan view transmission electron microscopy, Fourier transform infrared absorption, secondary ion mass spectroscopy, and four-point probe measurement of electrical conductivity. © 1999 American Institute of Physics.

[S0021-8979(99)09503-1]

I. INTRODUCTION

Polycrystalline silicon (polysilicon) is used extensively in the fabrication of thin film transistors (TFTs). Polysilicon formed by the crystallization of amorphous silicon (*a*-Si) has far superior material and electronic properties than as-deposited polysilicon^{1,2} due to the larger grains. The most commonly used method to crystallize *a*-Si is solid-phase crystallization (SPC), which requires annealing in a furnace at a maximum temperature of 600 °C for films on glass, or at higher temperature and shorter time in a rapid thermal annealer (RTA). Furnace annealing at 600 °C usually requires long anneal times of the order of 20–60 h.³ Various techniques have been tried to reduce the annealing time, including metal-induced crystallization (MIC),⁴ germanium-induced crystallization,⁵ and electron cyclotron resonance (ECR) oxygen and helium plasma enhanced crystallization.⁶ The latter process introduces the least contamination in the films, while the former two methods can lead to metal or germanium contamination of the films, respectively. We have found that a radio frequency (rf) hydrogen plasma exposure at room temperature of plasma-enhanced-chemical-vapor-deposited (PECVD) *a*-Si:H film can reduce this crystallization time by a factor of five⁷ compared to films not exposed to a plasma. This method was used for selective crystallization of *a*-Si:H, by using SiO₂ as a mask during plasma exposure.

In this article we describe the hydrogen plasma enhancement process and relate it to the structure of the *a*-Si:H film.

II. EXPERIMENTAL PROCEDURE

Hydrogenated amorphous silicon (*a*-Si:H) films of thickness from 150 to 400 nm were deposited on 7059 glass

substrates by PECVD in a parallel plate diode type chamber, using pure silane with flow rate of 50 sccm, chamber pressure of 500 mTorr, substrate temperatures of 150, 250, and 350 °C, and at rf power of ~0.02 W/cm². The subsequent rf plasma exposure was done in a parallel plate reactive ion etcher (RIE) at room temperature with hydrogen, oxygen or argon, with varying rf power and exposure times. The rf frequency was 13.56 MHz and the RIE electrode area was 250 cm². All samples were subsequently annealed in a furnace at 600 °C in N₂ for times ranging from 3 to 20 h. The UV reflectance spectrum⁸ of all samples was measured to monitor the crystallization process. Based on earlier work,⁸ the saturation of growth of the reflectance peak at 276 nm is used as an indication of complete crystallization of the sample. This was later confirmed by x-ray diffraction (XRD) and plan-view transmission electron microscopy (TEM). For the selective crystallization experiments, SiO₂ was deposited by electron beam evaporation and patterned by lithography and a dilute hydrofluoric acid etch. The SiO₂ was used to mask the plasma exposure to later realize polysilicon and amorphous silicon on the same substrate.

III. CRYSTALLIZATION OF PLASMA-TREATED FILMS

A. Introduction

Solid phase crystallization (SPC) of amorphous silicon (*a*-Si) involves two distinct processes, namely the nucleation of seeds (formation of clusters of crystalline silicon) and their growth to polycrystalline films. The rate-limiting step of the crystallization process is the rate of nucleation of seeds (r_n), which has an activation energy of about 5 eV.⁹ The rate of crystal growth (v_g) has an activation energy of about 2.7 eV.^{9,10} We will show that the plasma treatment hastens the crystallization and we suggest that this is due to the creation of seed nuclei, and hence the crystallization comprises only the growth of crystal from these seeds. It has

^{a)}Electronic mail: kpangal@ee.princeton.edu

^{b)}Electronic mail: sturm@ee.princeton.edu

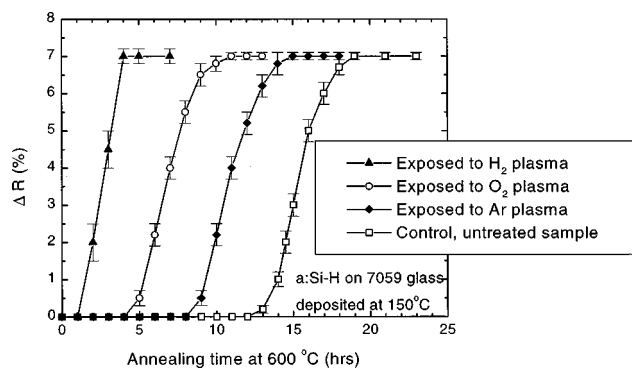


FIG. 1. Change in UV reflectance at 276 nm as a function of annealing time for samples exposed to different plasmas at rf power of 200 W for 90 min.

been previously reported⁶ that exposure to an electron cyclotron resonance (ECR) oxygen or helium plasma at substrate temperature of 300 °C results in the reduction of crystallization times. It has also been shown¹¹ that rf or ECR hydrogen plasma treatment at a substrate temperature of 300 °C of hot-wire *a*-Si:H films reduces the threshold laser power for crystallization of the films. In either case no explanation for the enhancement was given.

In our work, we studied the effect of hydrogen, oxygen, and argon plasmas on the crystallization of *a*-Si:H (Fig. 1). The rf power was 200 W, pressure 50 mTorr, and flow rate 50 sccm. A hydrogen plasma has the largest effect, with the total crystallization time, defined as the time taken to completely crystallize *a*-Si:H film, at 600 °C in N₂ ambient, reduced by a factor of five. Argon plasma had the smallest effect and oxygen plasma resulted in reduction of crystallization time by about two. The change in reflectance at 276 nm is used to monitor the degree of crystallization. As can be seen in Fig. 1, crystallization of the *a*-Si:H films as a function of annealing time, plasma treated or untreated, involves two distinct phases. During the first part, there is no crystallization and the UV reflectance peak at 276 nm is 0%, and this is the incubation period (τ_0). This is followed by the crystal growth period (τ_c), during which crystal growth occurs from the seed nuclei, and is characterized by growth of the UV reflectance peak at 276 nm and its ultimate saturation when the crystallization is complete. Figure 1 also shows that the plasma treatment reduces the incubation time with the crystal growth time being nearly constant.

B. Effect of annealing temperature

The total crystallization time of 150 nm *a*-Si:H films deposited at 250 °C on oxidized silicon substrates, either untreated or treated with hydrogen plasma at rf power of 200 W for 90 min, and annealed at different temperatures, is plotted in Fig. 2. As is expected, both curves exhibit similar characteristics, and the total crystallization time decreases as the annealing temperature is raised. A linear fit of the data yields an apparent activation energy of 3.7 eV for the untreated control sample, and 2.7 eV for the hydrogen-plasma-treated sample. These are not the actual activation energy of a single process as the total crystallization time includes incubation time (τ_0) and crystal growth time (τ_c). The two processes of

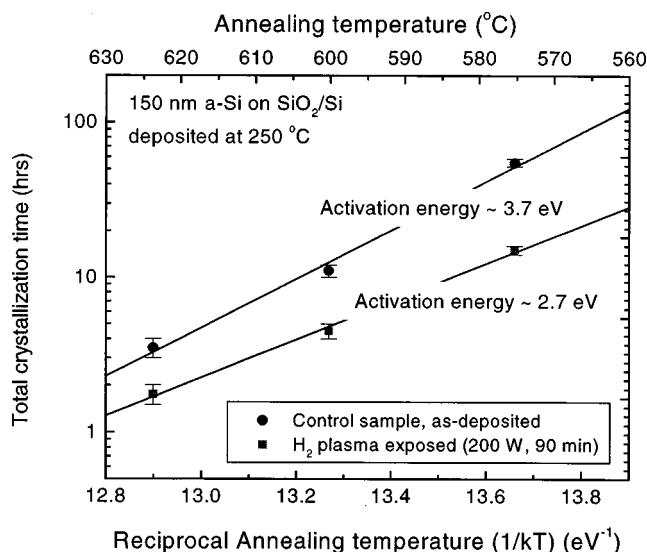


FIG. 2. Total crystallization time of *a*-Si:H films annealed as deposited or after hydrogen plasma treatment, as function of annealing temperature.

nucleation and crystal growth occur at the same time once a few seeds have formed. Separation of the crystallization time data of the various *a*-Si:H films into the basic processes is difficult and requires grain size and nucleation density data for different anneal times,⁹ which were not measured in this case. But the smaller activation energy of 2.7 eV for the hydrogen-plasma-treated sample, compared to 3.7 eV for the untreated control sample, indicates that the hydrogen plasma creates seed nuclei and that the crystallization time is the time taken for the seed nuclei to grow to a completely crystalline film.

C. Effect of rf power and exposure time

The total crystallization time falls as the rf power of the H₂ or O₂ plasma is increased as shown in Fig. 3(a). In either case, when the rf power is greater than 270 W, the plasma exposure leads to sputter etching of the film that produces pits and craters. The total crystallization time also becomes shorter as the plasma exposure time is increased and saturates after 60 min exposure in the case of H₂ and 180 min in the case of O₂ plasma exposure, respectively, as illustrated in Fig. 3(b).

D. Effect of deposition temperature

The total crystallization time also depends on the growth temperature of the *a*-Si:H films. The incubation time of crystallization increases as the growth temperature is reduced with the characteristic crystallization time being nearly constant. The total crystallization time falls linearly from ~17 to ~5 h for the untreated control sample as the growth temperature increases from 150 to 350 °C [Fig. 4(c)]. This correlates well with the total hydrogen content (as measured by IR absorption at 630 cm⁻¹) of the film, which also drops linearly from ~16.9 to ~8.5 at. % as the growth temperature increases from 150 to 350 °C [Fig. 4(a)]. Also, as the deposition temperature is lowered the IR absorption at 2000 cm⁻¹ corresponding to Si-H bonds¹² remains fairly constant,

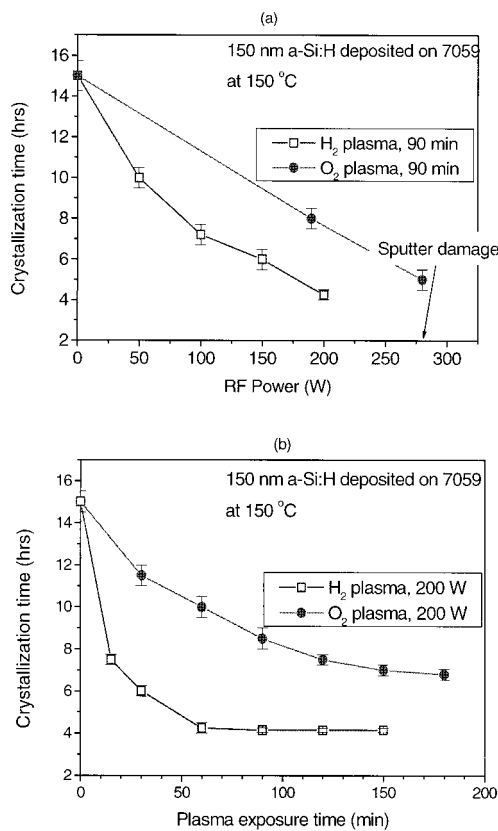


FIG. 3. Crystallization time of *a*-Si:H plasma treated samples as a function of (a) rf power and (b) exposure time, during exposure with chamber pressure of 50 mTorr and flow rate of 50 sccm.

while the IR absorption at 2090 cm^{-1} by Si-H₂ bonds^{12,13} increases as can be seen in Fig. 4(b). Therefore the increase in hydrogen content with decreasing growth temperature is due to the increase in silicon dihydride bonds.¹⁴ The total crystallization time of oxygen-plasma-treated samples [Fig. 4(c)] also drops as the deposition temperature increases, as does the crystallization time of the control samples. But the hydrogen-plasma-treated samples show no important change in total crystallization time with growth temperature [Fig. 4(c)], and in fact the total crystallization time increases from ~ 4 to ~ 5 h when the deposition temperature is raised from 150 to 250 °C, unlike the control samples. From this we infer that the number of incipient nucleation sites is increased as the PECVD growth temperature is raised. The relative constancy of the total crystallization time of the hydrogen-plasma-treated sample on deposition condition suggests that the seeding layer produced by the plasma treatment is the same regardless of starting conditions.

E. Effect of dopant in the film

The hydrogen plasma treatment also reduced the thermal budget for dopant activation. 280-nm-thick *in situ* phosphorus doped samples were deposited by PECVD on 7059 glass with a PH₃ flow of 6 sccm and a SiH₄ flow of 44 sccm, at chamber pressure of 500 mTorr, at substrate temperature of 240 °C, and rf power of $\sim 0.02\text{ W/cm}^2$. The phosphorus concentration in the film is $\sim 10^{20}\text{ cm}^{-3}$. These samples show the same crystallization trend as the intrinsic *a*-Si:H

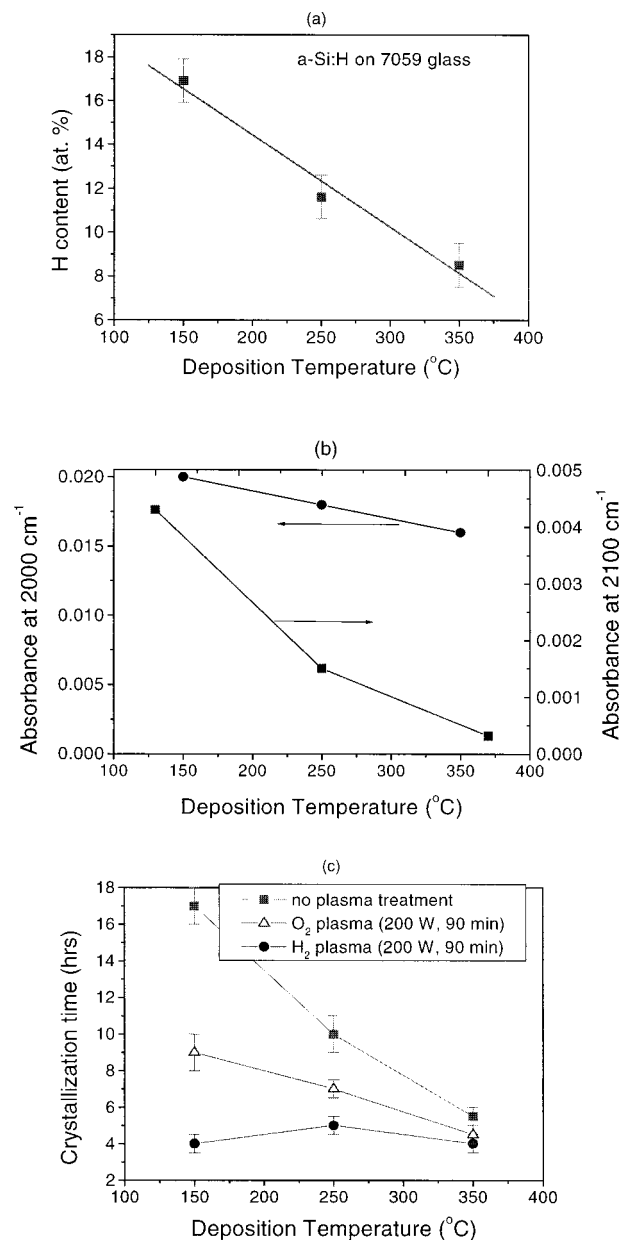


FIG. 4. (a) Hydrogen content in the *a*-Si:H film as a function of growth temperature, (b) IR absorbance at 2000 and 2100 cm^{-1} for *a*-Si:H films grown at different temperatures and, (c) crystallization time for plasma treated and untreated samples as a function of growth temperature.

films with the hydrogen plasma treatment reducing the dopant activation time from ~ 24 to ~ 4 h (Fig. 5). The ultimate sheet resistance ($\sim 25\ \Omega/\square$) after annealing at 600 °C in N₂ of the H₂-plasma-treated sample is the same as the untreated control sample.

F. Selective crystallization

To demonstrate selective crystallization, 100 nm of silicon dioxide (SiO₂) was deposited by *e*-beam evaporation on top of 150 nm of *a*-Si:H film deposited at 150 °C. The SiO₂ was then patterned and the samples were exposed to hydrogen plasma then all the remaining SiO₂ was stripped and the samples were annealed in the furnace. The exposed areas crystallized completely as expected, while the unexposed ar-

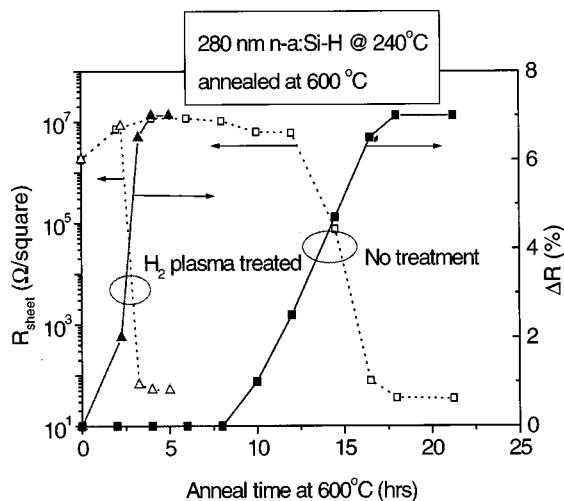


FIG. 5. Dopant activation and UV reflectance during annealing of a hydrogen plasma treated, and an untreated *a*-Si:H film doped with phosphorus at $\sim 10^{20} \text{ cm}^{-3}$ and grown at $\sim 240^\circ \text{C}$ on glass.

eas remain amorphous as can be seen in Fig. 6(a), and this was also confirmed by UV reflectance measurements. This shows that SiO₂ can mask against the effect of the plasma. Lateral crystallization does occur, however, with the crystal front growing out of the seeded (exposed) areas to the unexposed areas as can be seen in Figs. 6(b) and 6(c) with the lateral growth rate being $\sim 0.5 \mu\text{m/h}$ at 600°C .

G. Material characteristics of the films

The grains of completely crystallized (annealing at 600°C) 300-nm-thick *a*-Si:H films deposited at 150, 250, or 350°C , were predominantly oriented in the (111) vertical direction (Fig. 7) regardless of plasma treatment prior to SPC. Grains with (111) oriented surfaces predominate as the (111) plane has the least surface energy.¹⁵ The grain size of the polysilicon film as measured by TEM annealed without plasma treatment was $\sim 0.7 \mu\text{m}$, while the plasma treated and annealed samples had grains of about $0.4\text{--}0.5 \mu\text{m}$. Selective area diffraction of the films during TEM also confirmed that most of the grains had (111) orientation.

IV. MECHANISM OF SEEDING BY HYDROGEN PLASMA

A. Location of seed nuclei

In the preceding section we suggested that hydrogen plasma created seed nuclei which resulted in reducing the total crystallization time. In this section we determine the location of the seed layer and its composition. To test if the effect of the hydrogen plasma treatment on the crystallization occurred through a modification of only the surface of the amorphous silicon film, we dry etched the hydrogen-plasma-treated sample to various depths in a SF₆ plasma (rf power of 10 W, SF₆ flow rate of 15 sccm, and chamber pressure of 150 mTorr) before annealing. We then observed the effect of such etching on the crystallization time. To ensure that the SF₆ plasma itself did not affect the crystallization times, a control *a*-Si:H sample unexposed to any H₂

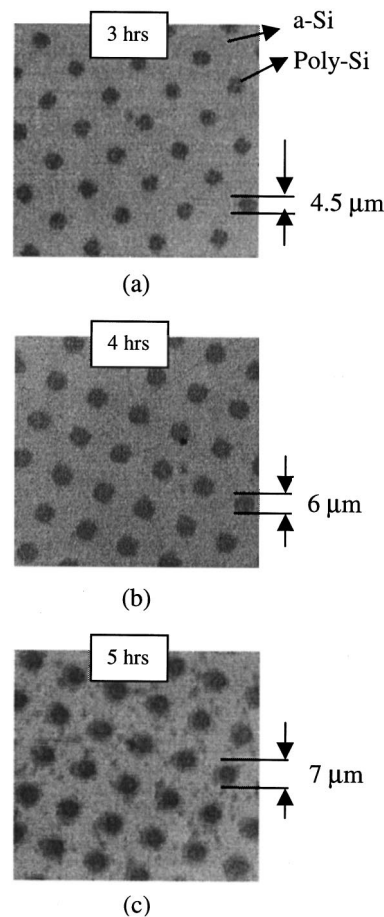


FIG. 6. (a) Optical micrograph showing selective crystallization with the dark areas ($\sim 4 \mu\text{m}$ diameter) being polycrystalline and the light areas being amorphous after 3 h of anneal, and (b) and (c) showing crystal growth around the seeded regions as samples were annealed at 600°C for 4 and 5 h, respectively.

plasma was etched at the same time and the crystallization times of this sample were also measured. All these control samples had the same crystallization time of $\sim 15 \text{ h}$, irrespective of the thickness of *a*-Si:H etched in the SF₆ plasma, hence demonstrating that the etch process itself does not affect the crystallization time. As can be seen in Fig. 8(a), a hydrogen-plasma-treated sample with the top $\sim 40 \text{ nm}$ thick layer removed crystallizes in the same time as an untreated sample. This proves that the surface region is responsible for rapid crystallization and that any seed nuclei are created in the top 30–40 nm layer. Figure 9 shows how the thickness of this seed layer varies with hydrogen plasma exposure time. The rf power was held constant at 200 W. Note also that the hydrogen plasma etches the film at a rate of $\sim 0.1 \text{ nm/min}$ at 200 W.

B. Possible structure of seed nuclei

Infrared absorption measurements of the untreated control samples and oxygen plasma treated samples of *a*-Si:H on silicon substrates show an absorption peak at 2000 cm^{-1} , but the hydrogen plasma exposed sample shows an additional peak at 2100 cm^{-1} , corresponding to the vibrational frequency of the Si–H₂ stretch mode¹² as can be seen in Fig.

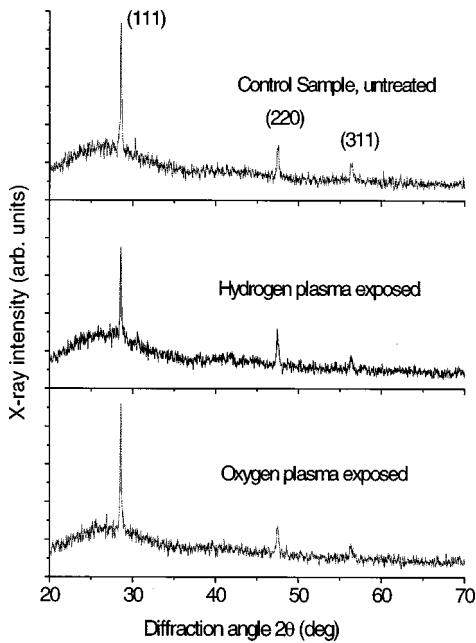


FIG. 7. X-ray diffraction of completely crystallized samples, as deposited or with prior hydrogen or oxygen plasma treatment, showing that the grains are predominantly oriented in the (111) direction.

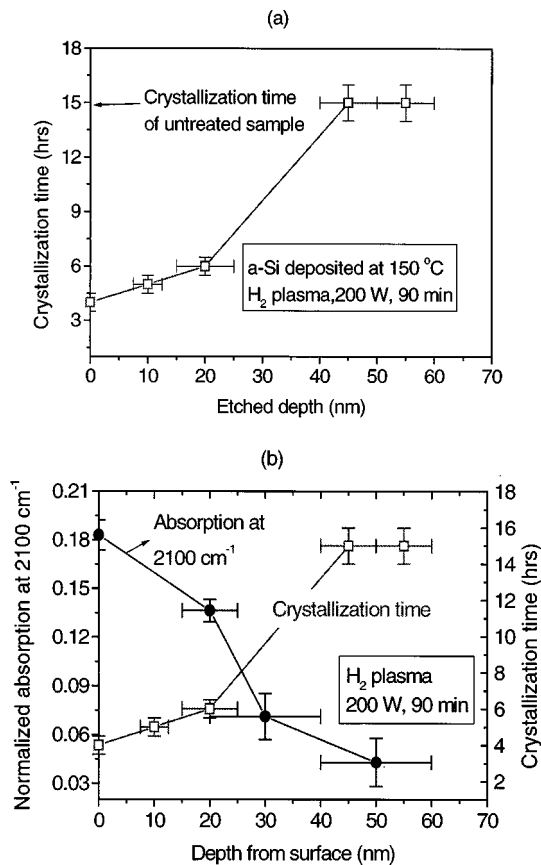


FIG. 8. (a) Crystallization time of samples etched to different depths by SF₆ plasma (20 W, 150 mTorr, and 15 sccm) after hydrogen plasma treatment at 200 W for 90 min, and (b) IR absorption at 2100 cm⁻¹ as function of depth from the surface for this sample.

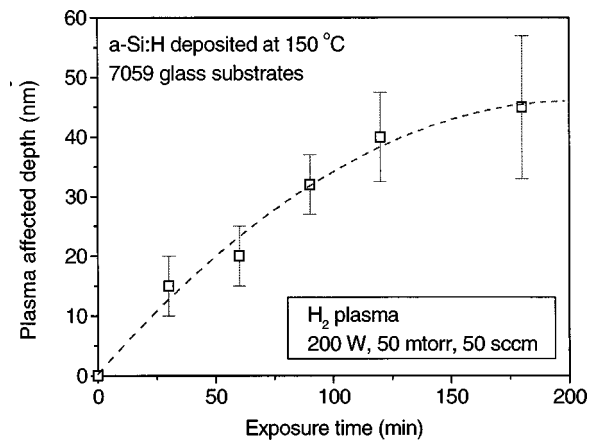


FIG. 9. Thickness of the plasma-modified layer as a function of exposure time to hydrogen plasma.

10. The appearance of the 2100 cm⁻¹ peak shows that hydrogen plasma treatment changes the microstructure of the *a*-Si:H film, producing Si-H₂ bonds. As the samples were progressively etched in the SF₆ plasma to increasing depths, the absorption peak at 2100 cm⁻¹ was reduced correspondingly. Figure 8(b) shows that this observation correlates well with the increase of the total crystallization time.

SIMS analysis of the films showed that the hydrogen plasma treatment also depletes hydrogen from the surface. This depletion effect is limited to a surface layer [Fig. 11(a)] whose thickness agrees well with the seed nuclei layer thickness as determined by progressive etching of the film, which we just discussed. The intensity of the Si-H stretch mode in the hydrogen-plasma-treated film, shown in Fig. 10, appears to suggest that the hydrogen content in the film increased after plasma treatment, in contrast to the SIMS data, but hydrogen content in *a*-Si:H films is most reliably calculated from the 630 cm⁻¹ peak, whose intensity is indeed consistent with the SIMS result. The hydrogen depletion effect is not as pronounced in *a*-Si:H films deposited at higher temperatures [Fig. 11(b)]. After a hydrogen plasma treatment at rf power

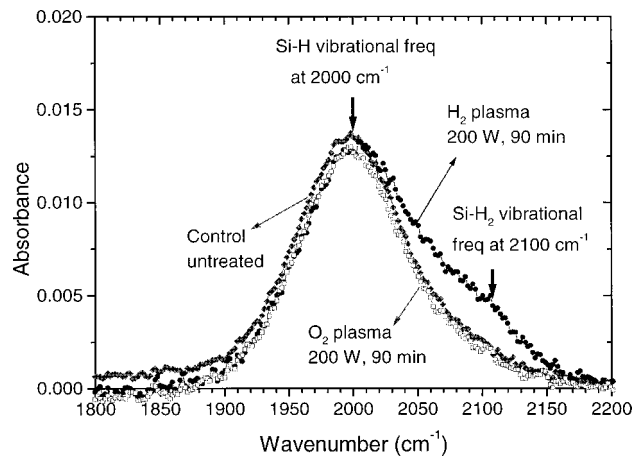


FIG. 10. The infrared spectra of *a*-Si:H films deposited at 250 °C, as deposited or hydrogen or oxygen plasma treated. The hydrogen plasma treated sample shows a shoulder at 2100 cm⁻¹ corresponding to Si-H₂ stretching mode.

of 200 W for 90 min the surface hydrogen concentration increased from 1×10^{19} to $8 \times 10^{19} \text{ cm}^{-3}$ for films whose growth temperature increased from 150 to 250 °C. In addition to hydrogen depletion, the hydrogen plasma treatment also leads to an increase in oxygen concentration at the surface of the *a*-Si:H as seen in Fig. 11(a).

SIMS also showed that the plasma treatment produced aluminum contamination, whose source is the aluminum oxide electrode plate that is getting sputtered onto the sample. (The $\sim 4 \text{ cm}^2$ samples were placed directly on an aluminum oxide coated electrode.) It is thought, however, that the concentration of aluminum ($\sim 10^{18} - 10^{17} \text{ cm}^{-3}$) at the surface of the sample is insufficient to cause any significant change in crystallization times.¹⁶ Typically the crystallization temperature for Al-Si alloys drops significantly for Al concentration of 4 at. % or higher. This was confirmed by placing the *a*-Si:H samples on a 100-mm-silicon wafer during exposure to plasma to reduce aluminum contamination to below 10^{17} cm^{-3} , which is the same as the untreated sample. These samples crystallized within the same time as the sample that was placed directly on the aluminum electrode.

C. Discussion

We are not aware of any work showing similar hydrogen depletion at the surface of *a*-Si:H film by hydrogen plasma treatment in another chamber after growth. However, there has been a series of work involving so-called chemical annealing in the PECVD growth chamber, whereby a thin *a*-Si:H layer is exposed to a hydrogen plasma or hydrogen radicals after the growth of the thin layer.¹⁷ This has been shown to cause depletion of hydrogen from the surface of *a*-Si:H film. Hydrogen is abstracted by the impinging H atoms, which interact with the silicon-hydrogen surface unit to form volatile H_2 molecules.^{18,19} It has been speculated that hydrogen abstraction is an important hydrogen elimination mechanism. Hydrogen abstraction is thought to lead to the formation of crystallites in the layer-by-layer growth of microcrystalline silicon ($\mu\text{c-Si:H}$), which involves alternating a SiH_4 plasma to deposit the *a*-Si:H film with a pure H_2 plasma to create microcrystallites of silicon in the surface layer. Similarly, the growth of $\mu\text{c-Si:H}$ by hydrogen dilution involves adding H_2 to SiH_4 during growth.¹⁸ This depletion will be more efficient if the silicon dihydride content in the film is higher, and in fact the formation of a porous SiH_n phase is an important step towards hydrogen induced crystallization.²⁰ As mentioned earlier, the films deposited at low temperatures (150 °C) have a higher dihydride content than films deposited at 250 °C, leading to higher hydrogen depletion from the surface of low-temperature films [Figs. 11(a) and 11(b)]. This could in turn lead to higher number of seed nuclei which explains why the crystallization time decreased from ~ 5 to ~ 4 h for the hydrogen plasma treated samples when the growth temperature was lowered from 250 to 150 °C. The infrared absorption spectra of $\mu\text{c-Si:H}$ films also show a peak at 2100 cm^{-1} ,²¹ because the microcrystallites of silicon embedded in an amorphous matrix are predominantly terminated by Si- H_2 bonds.^{18,21} This could explain why the hydrogen plasma treatment of the *a*-Si:H film

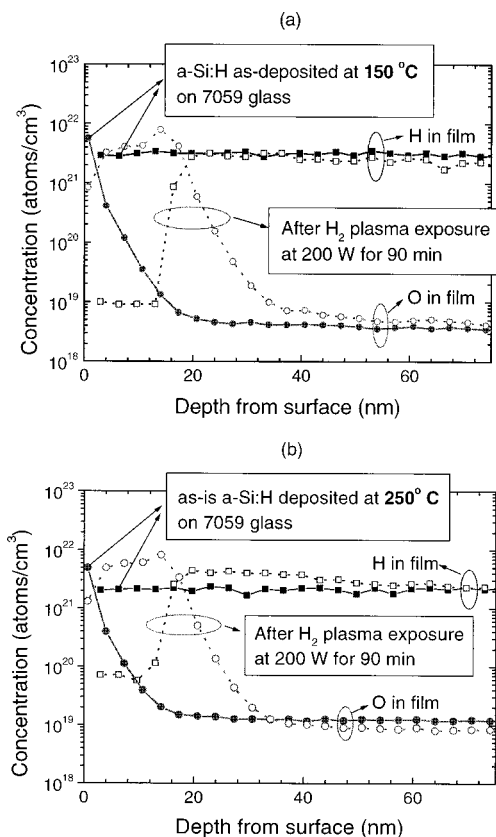


FIG. 11. (a) Hydrogen and oxygen concentration of *a*-Si:H films deposited at 150 °C before and after hydrogen plasma exposure, showing hydrogen depletion from the surface of the film, and (b) the same for film grown at 250 °C, showing less hydrogen depletion.

results in a peak at 2100 cm^{-1} , and why this microstructural change is limited to the top surface layer of the *a*-Si:H film.

Figures 11(a) and 11(b) show that the concentration of hydrogen at the surface of the *a*-Si:H film after the hydrogen plasma treatment is very low, suggesting that the top layer is nearly pure silicon in the form of a layer of silicon microcrystallites. The high concentration of oxygen in the films could be from post- H_2 plasma exposure to oxygen in the atmosphere, because hydrogen removal from the surface makes it extremely reactive and oxygen passivates the dangling bonds at the surface.²² The infrared absorption spectra, the crystallization time data, and the SIMS analysis of our samples are consistent with the fact that the hydrogen plasma treatment leads to the creation of small amounts of microcrystallites of silicon in the surface layer, which could then act as seeds during the subsequent crystallization process. While we have these indirect proofs for such an effect, we have not yet found the opportunity for experiments that could provide direct proof of the formation of microcrystallites of silicon such as Raman spectra with a peak at 522 cm^{-1} , or lattice plane imaging with high resolution TEM.

The nucleation of crystallites is also thought to be accelerated by both a rough surface and a porous *a*-Si:H with voids,²³ both of which in theory might be caused by the hydrogen plasma treatment. However, in our case the surface roughness induced by the hydrogen plasma was far less than (as measured by intensity of reflection of normal incidence

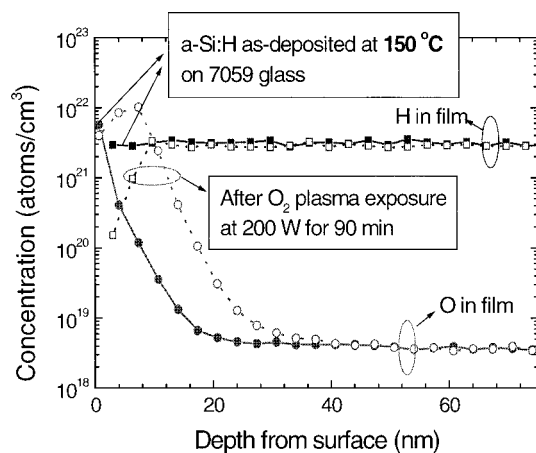


FIG. 12. Hydrogen and oxygen concentration of the *a*-Si:H film before and after oxygen plasma exposure, showing hydrogen abstraction from the surface of the film and the oxygen spike at the surface.

UV light) that induced by SF₆ plasma, (90% vs 20% of as-deposited *a*-Si:H films) which was used to etch the *a*-Si:H film. However, the SF₆ plasma treated film did not crystallize faster. It is possible, however, that any voids induced by the hydrogen abstraction, if any, and not microcrystallites of silicon led to the enhanced crystallization rate through faster nucleation of seeds.

V. OXYGEN PLASMA ENHANCED CRYSTALLIZATION

The oxygen plasma treatment also results in hydrogen abstraction from the surface of the *a*-Si:H films (Fig. 12), but the effect is not as pronounced as for the hydrogen plasma treatment and not as consistent, i.e., not all films exposed to oxygen plasma show this effect. The plasma exposure also leads to an increase in oxygen concentration at the surface as can be seen in Fig. 12. But this cannot be the reason for enhancement of crystallization as it is known that oxygen inhibits crystallization.²⁴ (This property is used to grow large grain polysilicon by incorporating oxygen at the *a*-Si/SiO₂ interface and thereby inhibiting nucleation at that interface.²⁵) Also, FTIR measurements of the oxygen plasma treated samples show no shoulder at 2100 cm⁻¹ unlike the hydrogen-plasma-treated samples. In the case of oxygen plasma treatment the reason for enhancement of crystallization is not yet clear. It is possible that trace amounts of hydrogen in the chamber (from water vapor) play a significant role by leading to hydrogen abstraction from the surface, which would explain the inconsistent results as this hydrogen amount might vary from run to run.

VI. CONCLUSION

Room temperature exposure to a rf hydrogen plasma can dramatically reduce the thermal budget for the crystallization of PECVD *a*-Si:H films. The hydrogen plasma treatment changes the microstructure of the *a*-Si:H at the surface, and

depletes hydrogen from the surface of the film. The plasma treatment probably creates seed nuclei of microcrystalline silicon or possibly voids. These seed nuclei enhance the overall crystallization rate. This technique can be used to reduce the thermal budget for the fabrication of polysilicon TFTs. This effect can be controlled spatially resulting in polycrystalline silicon and amorphous silicon areas on the same substrate.

Note added in Proof: Similar enhanced crystallization data to that in Fig. 1 to a *high temperature* (400 °C) hydrogen ECR plasma treatment have also been reported in US Patent 5624873, 1997.

ACKNOWLEDGMENTS

This work was supported by DARPA through ONR under Contract No. N66001-97-1-8904 and the Princeton Program in Plasma Science and Technology (DOE Contract No. DE-AC02-76-CHO-3073). We appreciate the reviewer's comments pointing to the possible importance of surface porosity.

- ¹R. A. Ditzio, G. Liu, and S. J. Fonash, *Appl. Phys. Lett.* **56**, 1140 (1990).
- ²K. H. Milliadis, *J. Appl. Phys.* **63**, 2260 (1988).
- ³E. Korin, R. Reif, and B. Mikic, *Thin Solid Films* **167**, 101 (1988).
- ⁴R. J. Nemanich, C. C. Tsai, M. J. Thompson, and T. W. Sigmon, *J. Vac. Sci. Technol.* **19**, 685 (1981).
- ⁵D. K. Sadana, E. Myers, J. Liu, T. Finstad, and G. A. Rozgonyi, *Mater. Res. Soc. Symp. Proc.* **23**, 303 (1984).
- ⁶A. Yin, S. J. Fonash, D. M. Reber, Y. M. Li, and M. Bennett, *Mater. Res. Soc. Symp. Proc.* **345**, 81 (1994).
- ⁷K. Pangal, J. C. Sturm, and S. Wagner, *Mater. Res. Soc. Symp. Proc.* **507** (1998).
- ⁸A. Yin and S. J. Fonash, *Tech. Dig. IEEE Electron. Devices Mtg.* 397 (1993).
- ⁹R. B. Iverson and R. Reif, *J. Appl. Phys.* **62**, 1675 (1987).
- ¹⁰L. Csepregi, E. F. Kennedy, and J. W. Mayer, *J. Appl. Phys.* **49**, 3906 (1978).
- ¹¹J. P. Conde, P. Brogueira, and V. Chu, *Mater. Res. Soc. Symp. Proc.* **452**, 779 (1997).
- ¹²C. C. Tsai and H. Fritzsche, *Sol. Energy Mater.* **1**, 29 (1979).
- ¹³G. Lucovsky, R. J. Nemanich, and J. C. Knights, *Phys. Rev. B* **19**, 2064 (1979).
- ¹⁴M. H. Brodsky, M. Cardona, and J. J. Cuomo, *Phys. Rev. B* **16**, 3556 (1977).
- ¹⁵C. V. Thompson and H. I. Smith, *Appl. Phys. Lett.* **44**, 603 (1984).
- ¹⁶G. Radnoczi, A. Robertsson, H. T. G. Hentzell, S. F. Gong, and M. A. Hasan, *J. Appl. Phys.* **69**, 6394 (1991).
- ¹⁷H. Shirai, D. Das, J. Hanna, and I. Shimizu, *Appl. Phys. Lett.* **59**, 1096 (1991).
- ¹⁸E. Srinivasan and G. N. Parsons, *J. Appl. Phys.* **81**, 2847 (1997).
- ¹⁹M. Otake and S. Oda, *Jpn. J. Appl. Phys., Part 1* **31**, 1948 (1992).
- ²⁰C. Godet, N. Layadi, and P. Roca i Cabarrocas, *Appl. Phys. Lett.* **66**, 3146 (1995).
- ²¹S. Ray, S. C. De, and A. K. Barua, *Thin Solid Films* **156**, 277 (1988).
- ²²R. A. Street, *Hydrogenated Amorphous Silicon* (Cambridge University Press, London, 1991), p. 334.
- ²³P. Roca i Cabarrocas, S. Hamma, and A. Hadjadj, *Appl. Phys. Lett.* **69**, 529 (1996).
- ²⁴E. F. Kennedy, L. Csepregi, J. W. Mayer, and T. W. Sigmon, *J. Appl. Phys.* **48**, 4241 (1977).
- ²⁵M. K. Ryu, S. M. Hwang, T. H. Kim, and K. B. Kim, *Appl. Phys. Lett.* **71**, 3063 (1997).